CHEMICAL ENGINEERING TRANSACTIONS
VOL. 117, 2025
A publication of AIDIC
The Italian Association of Chemical Engineering
Online at www.cetjournal.it
Guest Editors: Fabrizio Bezzo, Flavio Manenti, Gabriele Pannocchia, Almerinda di Benedetto

ISBN 979-12-81206-17-5; **ISSN** 2283-9216
DOI: 10.3303/CET25117206

Optimising Extrusion-Based Pla-Asa 3D Printed Drug Delivery Mesh using Pat Tools

Yazan Odeh[a], Debleena Mitra[b], Mohammad O. A. Malik[b], Douglas R Marques[a], Rabah Mouras[b], Marion McAfee[a*]

[a]Center for Mathematical Modelling and Intelligent Systems for Health and Environment (MISHE), Atlantic Technological University, ATU Sligo, Ireland
[b]Pharmaceutical Manufacturing Technology Center (PMTC), University of Limerick, Ireland
Yazan.odeh@research.atu.ie

In this study, the use of extrusion-based 3D printing for the fabrication of a personalized drug delivery Polylactic acid (PLA) – Aspirin (ASA) mesh for bone tissue engineering is examined. Hot Melt extrusion (HME) significantly improves the solubility and bioavailability of poorly soluble drugs, while 3D printing enables personalised drug dosage, geometry, and mechanical properties. PLA is biodegradable and has properties that allow cellular attachment and tissue regeneration; while ASA is a substance that promotes bone regeneration and decreases associated infections. Surgical meshes for bone tissue repair and drug delivery are created through Hot Melt Extrusion (HME) and Fused Deposition Modelling (FDM) 3D printing. This work investigates the production of PLA-ASA filament using a low-cost single-screw filament extruder, the effects of 3D printing temperature on ASA stability using Raman Spectroscopy, and the flexibility and integrity of 3D printed PLA-ASA mesh.

1. Introduction

Controlled release of therapeutic agents from drug delivery systems is important for many modern treatment regimes. Traditional drug delivery strategies have inherent limitations including burst release, poor bioavailability, and side effects of systemic drug exposure. Due to these challenges, there has been escalating interest in advanced drug delivery implants providing localised, sustained and controlled release profiles (Tambe et al., 2021). Personalized drug delivery devices have been fabricated with control over geometry, internal structure, and drug distribution, using three-dimensional (3D) printing technology (Bácskay et al. 2022). Surgical meshes have traditionally been used to provide mechanical support to tissues, however advanced devices actively participate in the healing process by also providing localized therapeutic delivery. Active pharmaceutical ingredients (API) can be incorporated directly into the mesh during manufacturing. Literature reveals that these meshes can provide controlled drug release profiles in the context of appropriate mechanical properties that meet the needs of native tissue (Corduas, F. et al 2023). Their dual functionality as both a drug delivery vehicle and for structural support makes them desirable for surgical applications where tissue reinforcement and drug delivery are both necessary for a successful outcome (Ivanovski. et al 2023). PLA has garnered a lot of attention among the array of biodegradable materials used in pharmaceutical 3D printing due to biocompatibility, thermal stability, and mechanical properties (Arif. et al 2022). Concerning the API, beyond its conventional use in anti-inflammatory therapy, ASA possesses multiple therapeutic potentials for bone tissue engineering. By activating osteoblast–related cytokines, it promotes bone regeneration (Fattahi.et al 2022). A key roadblock for personalised drug delivery systems is achieving satisfactory quality assurance protocols to ensure patient safety. Regulatory authorities recommend Process Analytical Technology (PAT) tools which will allow real-time monitoring and control of critical quality attributes during the manufacturing process (Ervasti et al., 2020). These tools, first and foremost, enable practitioners to implement Quality by Design (QbD) principles and to ensure that products will be consistent in quality throughout their lives (Munir et al., 2024). By integrating PAT tools into the fabrication process it is possible to continuously monitor critical process parameters, including extrusion temperature, filament diameter and drug degradation, all of which directly affect drug stability, release kinetics,

Paper Received: 3 December 2024; Revised: 3 April 2025; Accepted: 30 May 2025
Please cite this article as: Odeh Y., Mitra D., Malik M.O.A., Marques D.R., Mouras R., Mcafee M., 2025, Optimising Extrusion-based Pla-asa 3D Printed Drug Delivery Mesh Using Pat Tools, Chemical Engineering Transactions, 117, 1231-1236 DOI:10.3303/CET25117206

and mesh mechanical properties (Munir et al., 2021). This research focuses on the correlation between processing parameters and critical quality attributes, and the prospect of using real-time monitoring systems to ensure the quality of drug delivery devices which are custom manufactured by 3D printing.

2. Materials and Methods

Polylactic acid (PLA) pellets (INGEO BIOPOLYMER 4043D) were obtained from Nature Works LLC. Acetylsalicylic acid (ASA) with ≥99.0% purity was supplied by Sigma-Aldrich. The materials were carefully weighed and combined in a ratio of 80:20% w/w (PLA: Aspirin). The polymer/API mixture underwent the pre-processing step of controlled drying at 65°C for 3 h to remove any residual moisture. The dried powder components were then mixed using a mortar and pestle and further blended via manual bag mixing to ensure thorough mixing and uniform distribution of the API throughout the polymer matrix. The resulting blend was sealed under controlled storage conditions using a desiccator to avoid moisture uptake prior to extrusion. A PLA-ASA filament was produced using a single screw hot melt extruder (3D Evo B.V., The Netherlands) equipped with a laser micrometre for real-time diameter monitoring, and an auto-spooling system. Auto calibration of the spooling system was selected to achieve printable filament dimensions in the range of 1550 mm Lower limit (Green) and 1850 mm Upper limit (Red). A portable Raman spectroscopy system with a 1064 nm laser (Ocean Optics) was utilised to analyse the composition of the blend and extruded filament to assess checking for degradation of the ASA. The extruded filament was dried at 45°C for 6 h with a desiccator and stored in a heat-sealed bag to avoid any moisture prior to 3D printing. The filament was subsequently employed in an FDM 3D printer (Prusa MK3) to build the STL file made using Prusa Slicer. The mesh shape was designed using SolidWorks and Prusa Slicer software. The mesh was designed to have a gyroid pattern infill. Separately, a Serpentine pattern g-code was manually edited to have a modified temperature profile per vertical block to investigate the effect of nozzle temperature on the ASA stability. The printed objects were then removed carefully and placed in a sealed desiccated bag. Raman spectroscopy was also carried out post-printing using a LabRAM HR Evolution (HORIBA UK Ltd.) in a backscatter configuration with 785 nm excitation, and an acquisition time of 5s for 2 accumulations. Spectra were collected using a 10× objective at a 4 cm^{-1} resolution, over scan ranges of 100–3400 cm^{-1} using 600 g/mm grating. UV-Vi's spectroscopy analysis was conducted using The Cary 60 UV-Vis Spectrophotometer. The wavelength range used was 200-500 nm. 10 grams of the material from each section was diluted in 50 millilitres of ethyl acetate. Samples were subjected to sonication for 30 minutes at 30°C and subsequently filtered using a 20 µm syringe filter.

3. Results and Discussion

3.1 PAT tools and inline monitoring:

Extruder zone temperature settings were selected following initial screening studies. Extruder zones are numbered 1 (die end) to 4 (feeding end). These studies highlighted that the zone 3 temperature is critical, with obvious degradation and poor filament quality at temperatures above 150°C. A high die temperature however helped achieve a smooth filament surface. While a high screw speed is desirable to reduce the residence time of the API in the extruder, at screw speeds of 10rpm again poor filament quality was observed, with variable diameter, high surface roughness and discoloration. The selected settings were, screw speed of 7rpm, and temperature profile from zone 4 to zone 1: Ambient temperature - 135°C - 150°C - 165°C. A compilation of real-time data collected by 3D Evo software is displayed in Figure 1. In some cases, the actual temperature in the extruder barrel zones diverged from the set-point temperature, particularly in zone 3 where the temperature was significantly higher than the set point, indicating limitations in the temperature control of the machine. An analysis of filament thickness variability over time is shown in Figure 2. This shows the measured filament thickness taken at regular intervals (1 second) throughout the extrusion process. Statistical evaluation reveals a mean thickness of 1745.0 µm, a standard deviation of 78.9 µm and a coefficient of variation (CV) of 4.5%. High variability exists in filament thickness indicated by the presence of frequent peaks and valleys in the thickness data coupled with red data points being above the specification and green data points below the specification. The inconsistency in the filament dimensions may be due to various reasons including uneven melting, chatter in the spooling mechanism, and sensor noise. The data demonstrate that the extrusion process is not consistent as is, and that there are areas for improvement in controlling the variables that contribute to filament thickness. Figure 3 displays a 20-point running average of the thickness of the filament that occurs during the extrusion process. It can be seen that as the zone 3 temperature comes closer to the set point over time the filament diameter becomes more consistent.

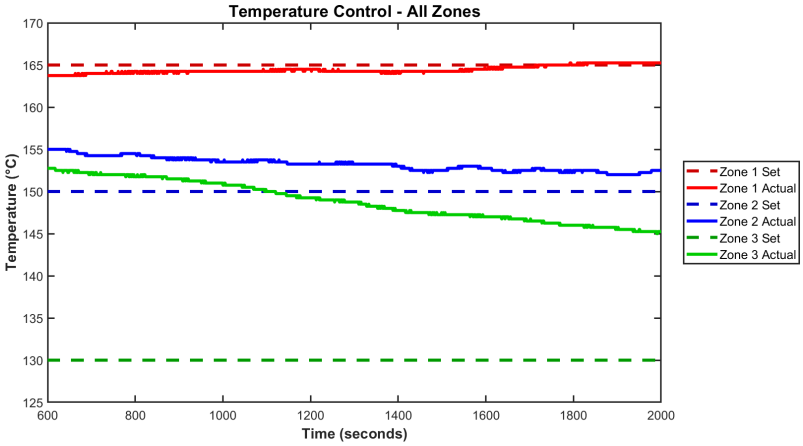

Figure 1 Temperature variations across the extruder. Starting with Zone 4 (Feeding zone)

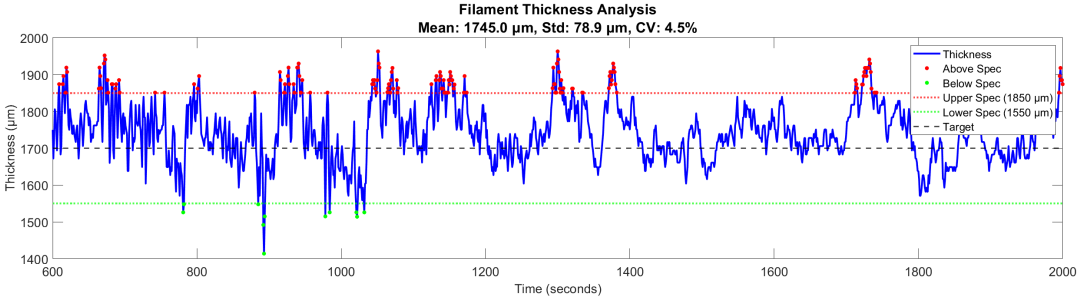

Figure 2 Filament Thickness Analysis. Red line indicates the Upper control limit and green line indicate the lower control limit

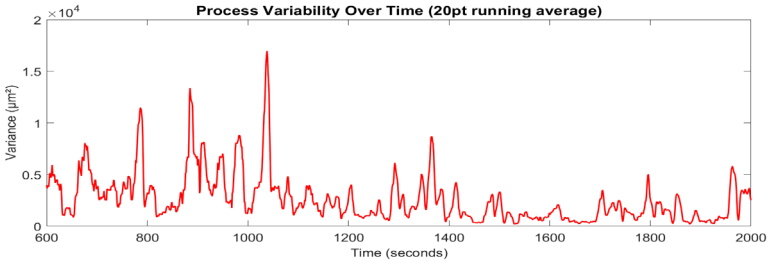

Figure 3 Process stability

3.2 Effect of Printer Nozzle Temperature on PLA/ASP blend

An initial PLA-ASA print was carried out using varying nozzle temperatures to create the serpentine pattern shown in Figure 7. Each column in the shape was printed at a different nozzle temperature, with the horizontal bridges allowing the nozzle temperature time to reach the new target temperature. Pure PLA powder and the final 3D printed mesh (Figure 6 (B)) were analysed with Raman Spectrometry. The following characteristic peaks were observed pre-extrusion and post-3D printing (Figure 4) around 1774 cm^{-1} which can be described C=O stretching, CH_3 deformation around 1454 cm^{-1} and the vibration of C-COO around 870 cm^{-1}(Bolskis et al., 2022). In both pure Aspirin spectra and the 3D printed mesh, the characteristic ASA peak of the aromatic ring, was observed at 1607 cm^{-1}[12]. Moreover, the confocal Raman map (figure 4) shows a distribution of aspirin peaks around 1605 cm^{-1} (green), compared to PLA-related CH_3 peaks around 1454 cm^{-1} (red) at 200°C. These results show the presence of the API within the matrix of PLA, however, the analysis of a single peak is limited, and it is possible the 1605 cm^{-1} peak could be related to salicylic acid,a degradation product of ASA. UV-Vis analysis of aspirin and 3D printed samples (Figure 5), shows no signs of aspirin in the mesh sample but shows a small presence of salicylic acid. This can be explained by hydrolysis of aspirin, although this can also occur in the process of dissolving in ethanol to perform the UV-Vis analysis.

Further Raman analysis was conducted on each column (Figure 6(A)) to examine the stability of the ASA at a single peek 1607 cm^{-1} under different nozzle temperatures resulting in the spectra shown in Figure 7(B). The plot of the intensity of the peak in the region 1600–1620 cm^{-1}as a function of temperature (Figure 8) shows that this peak intensity decreases as the temperature is increased from 200 to 220°C, thus suggesting degradation of ASA at a higher temperature. The measurements show a negative rate of change -2.85%/°C and a total change of -55.7% of the peak intensity between the printing temperature of 200 to 220°C. Therapeutic ability and bioavailability can be expected to decrease significantly as a result of thermal degradation. Further testing could quantify this degradation against industry standards (Crowell et al., 2015). Therefore, these findings highlight how critical it is to carefully control the extrusion temperature to limit Aspirin loss by degradation as well as to ensure high drug loading in the final product. The 3D printed mesh (Figure 6(B)) shows an elastic behaviour despite PLA typically being known for its stiffness. These results confirm the plasticising effect of Aspirin on PLA as reported in other studies (Chomcharn et al., 2013). The enhanced flexibility enables the material to be used in regions that require conformability. The use of Raman spectroscopy data confirms the successful integration of Aspirin in the PLA matrix during extrusion. Raman analysis of the PLA-ASA printed at different temperatures shows degradation of Aspirin that depends on temperature requiring close temperature control. It shows that Aspirin, as a plasticizer of PLA, improves the flexibility of the manufactured mesh.

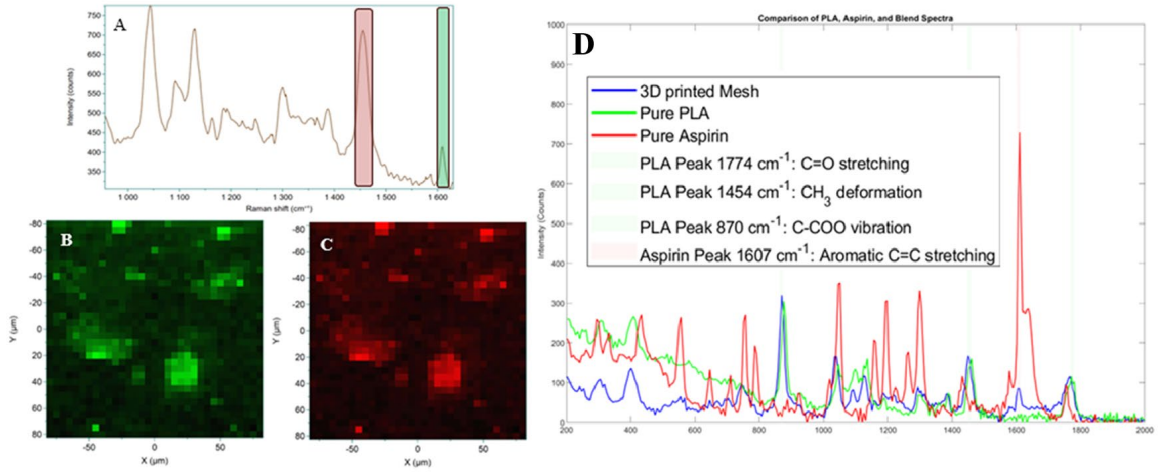

Figure 4 A) Confocal Raman map (785 nm), A) selected ASA peaks around 1605 cm^{-1} (green), compared to PLA-related CH_3 peaks around 1454 cm^{-1} (red) at 200°C. B) Aspirin (Green), C) PLA (Red) D) PLA, Aspirin, 3D printed Mesh Raman shift using (1064 nm Raman).

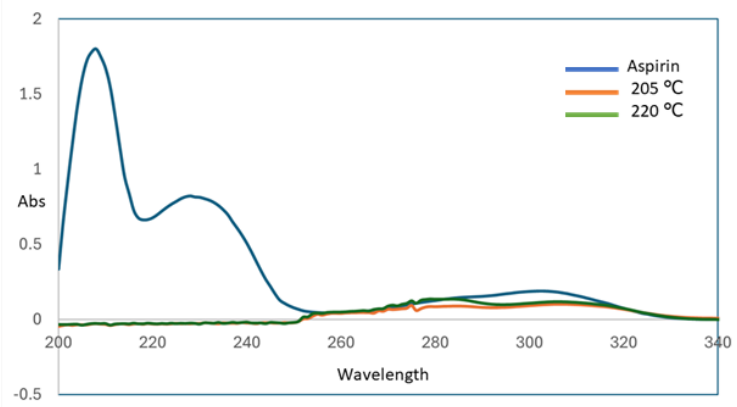

Figure 5 UV-Vis Spectrum of Aspirin and 3D printed samples.

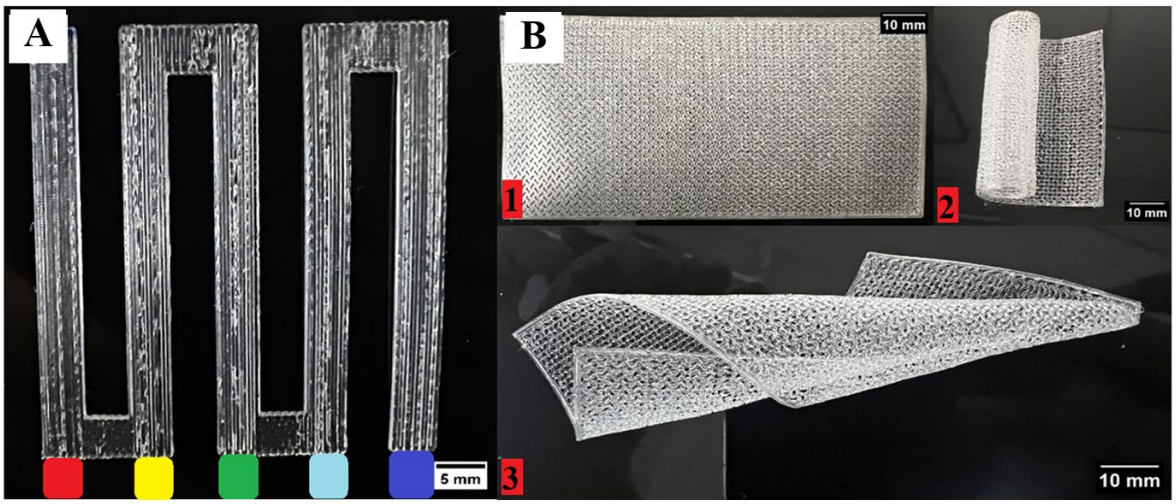

Figure 6 A) 3D printed Serpentine pattern. Starting from left (Highest temperature 220°C Orange) to the right (lowest temperature 200°C Blue). A decrement of 5°C degree was applied in the G-Code to print this design. B) 3D printed mesh. 1) Flat, 2) Rolled, 3) Twisted.

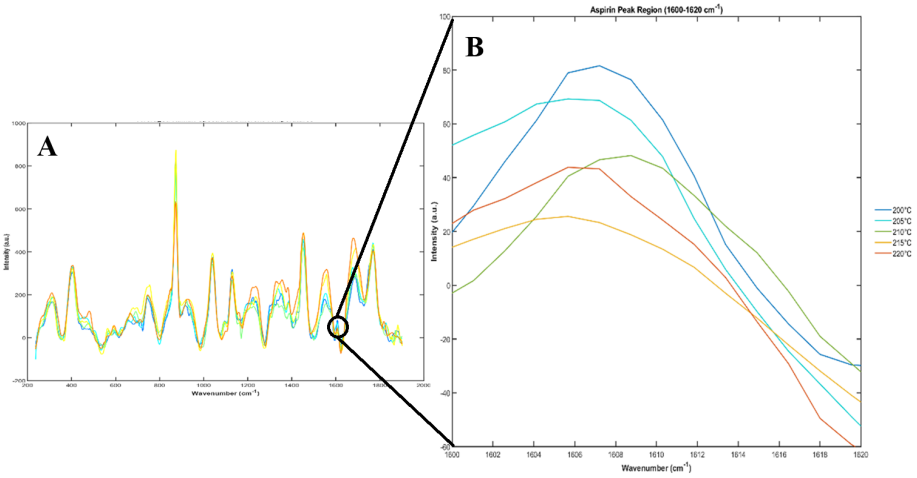

Figure 7 A) Raman spectra of serpentine pattern using different printing temperatures (200°C in Blue), (205°C in sky blue), (210°C in green), (215°C in Yellow), and (220°C in orange). B) Aspirin aromatic ring close view at region of 1600-1620 cm⁻¹.

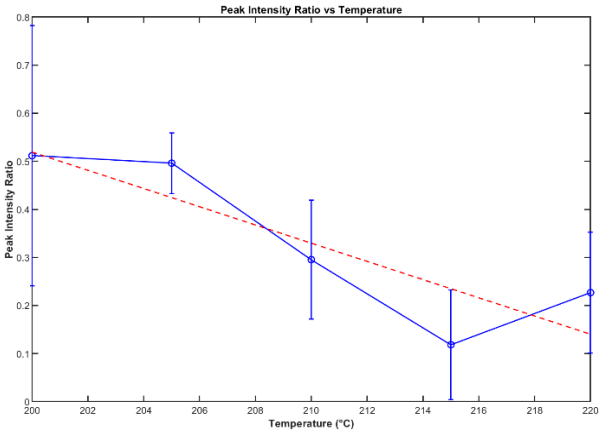

Figure 8 Aspirin peak intensity ratio vs temperature.

4. Conclusion

The development of drug loaded personalised implants can open new opportunities in tissue engineering, regenerative medicine, material science, and other fields. The study focused on highlighting the importance of having PAT tools in line to monitor the quality of extruded filaments and 3D printed implants. Raman analysis was used to understand the effect of printing temperature on the intensity of API and polymer peaks. The results showed a possible relation between the temperature fluctuation and filament diameter, however the filament was printable despite the fluctuations in the filament diameter. It was shown that the nozzle temperature has an impact on degradation of the Aspirin during the 3D printing process, having higher degradation rate with higher temperature. The blend of PLA/Aspirin showed an elastic mechanical property that can be advantageous for conforming the mesh to specific patient requirements. These findings demonstrate that extrusion-based 3D printing may prove suitable for creating personalised drug delivery meshes for tissue engineering, but the complexity of such a process is beyond standard consumer-grade 3D printers and filament extruders. The technical challenges encountered in processing parameters, material properties and drug incorporation effects are such a complex interplay that advanced manufacturing solutions must be applied. PAT tools have a critical role in the quality monitoring of personalised drug delivery devices. Further research is needed to achieve a robust interpretation of API degradation by Raman spectroscopy.

Acknowledgements

This publication has emanated from research conducted with the financial support of Research Ireland under grant number 21/FFP-A/0152. For the purpose of Open Access, the *authors have* applied a CC BY public copyright licence to any Author Accepted Manuscript version arising from this submission.

References

Arif Z.U., Amin P., Jain D., Agarwal Y., 2022, Recent advances in 3D-printed polylactide and polycaprolactone-based biomaterials for tissue engineering applications, International Journal of Biological Macromolecules, 218, 930–968.

Bácskay I., Ujhelyi Z., Fehér P., Arany P., 2022, The evolution of the 3D-printed drug delivery systems: A review, Pharmaceutics, 14.

Bolskis E., Adomavičiūtė E., Griškonis E., 2022, Formation and investigation of mechanical, thermal, optical and wetting properties of melt-spun multifilament poly(lactic acid) yarns with added rosins, Polymers (Basel), 14.

Chomcharn N., Xanthos M., 2013, Properties of aspirin modified enteric polymer prepared by hot-melt mixing, International Journal of Pharmaceutics, 450, 259–267.

Corduas F., et al., 2021, Melt-extrusion 3D printing of resorbable levofloxacin-loaded meshes: Emerging strategy for urogynaecological applications, Materials Science and Engineering C, 131.

Crowell E.L., Dreger Z.A., Gupta Y.M., 2015, High-pressure polymorphism of acetylsalicylic acid (aspirin): Raman spectroscopy, Journal of Molecular Structure, 1082, 29–37.

Ervasti T., et al., 2020, The comparison of two challenging low dose APIs in a continuous direct compression process, Pharmaceutics, 12.

Fattahi R., Mohebichamkhorami F., Khani M.M., Soleimani M., Hosseinzadeh S., 2022, Aspirin effect on bone remodeling and skeletal regeneration: Review article, Tissue and Cell, 76.

Ivanovski S., et al., 2023, 3D printing for bone regeneration: challenges and opportunities for achieving predictability, Periodontology 2000, 93, 358–384.

Munir N., De Lima T., Nugent M., McAfee M., 2024, In-line NIR coupled with machine learning to predict mechanical properties and dissolution profile of PLA-Aspirin, Functional Composite Materials, 5(1), 14.

Munir N., Nugent M., Whitaker D., McAfee M., 2021, Machine learning for process monitoring and control of hot-melt extrusion: Current state of the art and future directions, Pharmaceutics, 13.

Tambe S., Jain D., Agarwal Y., Amin P., 2021, Hot-melt extrusion: Highlighting recent advances in pharmaceutical applications, Journal of Drug Delivery Science and Technology, 63, 102452.